Acta Neurologica Belgica (2023) 123:1861–1868
https://doi.org/10.1007/s13760-022-02097-7

ORIGINAL ARTICLE

Evaluation of anterior and middle cranial fossa intraosseous arachnoid granulations with 3D T2-SPACE sequence

Elif Gozgec[1] · **Hayri Ogul**[1] · **Hasan Durmus**[1]

Received: 11 April 2022 / Accepted: 12 September 2022 / Published online: 2 October 2022

Abstract

Objectives Arachnoid granulations (AG) can be located anywhere outside the dural sinuses. Their presence is thought to be associated with idiopathic intracranial hypertension (IIH) and cerebrospinal fluid (CSF) leaks. It was aimed to evaluate the intraosseous AGs located in the middle and anterior cranial fosses in detail with three-dimensional T2-SPACE (Sampling Perfection with Application optimized Contrasts using different flip angle Evolution—Siemens) imaging and to investigate their clinical significance.

Materials and methods Sixty-five intraosseous AG of 46 patients were included in this retrospective study. The highest diameter, bone indentation degree (in the inner tabula, diploe distance, reaching and exceeding the outer tabula), content (CSF/+parenchyma) of each AG were evaluated by 2 experienced radiologists. In addition, the presence of other MRI findings supporting IIH was examined.

Results Additional signs of IIH were detected in 25 patients, and they were statistically significantly more common in the middle cranial fossa. Parenchymal herniation (in four patients) was more common in the young population.

Conclusions Intraosseous AGs can be evaluated in detail with T2-SPACE imaging. Determining intraosseous AG is very important both as an indicator of IIH and in terms of its content. T2-SPACE imaging is superior to CT and conventional sequences in this regard.

Keywords MR imaging · Arachnoid granulations · T2-SPACE · Intraosseous

Introduction

Arachnoid granulations (AGs) are anatomical structures that are the transition points of the cerebrospinal fluid (CSF) to the venous system [1, 2]. Although they most commonly extend along the sagittal and transverse sinuses, they can occur anywhere else unrelated to the venous structures [3, 4]. They can range in size from a few millimeters to over 1 cm. They are usually pits containing CSF, but particularly large ones may also contain the brain parenchyma [1, 5]. Their indentations to the adjacent bone structure can vary from the inner table to the outer table. CSF leaks can occur when the bone structure is completely destroyed. In particular, AGs in the middle cranial fossa (MCF) are also called arachnoid pits. These are associated with increased intracranial pressure (ICP) and are counted among the radiological findings of increased ICP, as well as empty sella, optic nerve sheath anomalies, dural ectasia, enlargement of Meckel's cave and meningoencephalocele [6–8].

Osseous arachnoid granulations are recognized by having the same density as CSF in computed tomography (CT). However, it is difficult to make a differential diagnosis with many tumoral lesions such as metastasis, multiple myeloma and hemangioma, especially those that extend to the outer table and are numerous. In conventional cranial magnetic resonance (MR) sequences, AGs are recognized as having similar content to CSF and being well defined. Signal characteristics may vary in AGs containing parenchyma, which may make the diagnosis difficult [9, 10].

Three-dimensional T2-SPACE (Sampling Perfection with Application optimized Contrasts using different flip angle Evolution—Siemens) technology for MR imaging will be tried and selected for the first time by Mugler et al. [11]. The name of the sequence in question varies depending on the scanner (VISTA-Philips, CUBE-GE). It provides

✉ Elif Gozgec
elf.gvn@hotmail.com

[1] Ataturk University, Yakutiye, Turkey

higher resolution images and provides anatomical detailed information compared to the sequences used in the routine. This multi-planar imaging reduces the partial volume effect and provides high spatial resolution images. Due to its high motion sensitivity, CSF flow dynamics and black blood can be evaluated. It is used in the evaluation of hydrocephalus patients, CSF leakage, craniocervical pseudomeningocele, third ventriculostomy patency, cervical spine anatomy, and localization of spinal dural arteriovenous fistula [11–13].

The aim of this study was to investigate the value of T2-SPACE imaging in the detailed evaluation of intraosseous AGs about the contents and level of bone indentation (Fig. 1). In addition, we aimed to investigate the other radiological findings of ICP increase in a single sequence and evaluate its relationship with intraosseous AG.

Materials and methods

Patients

Consecutive patients who applied to our hospital and underwent cranial MRI between January 2020 and December 2020 were included in this retrospective study. Ethics committee approval was obtained (ethics review number 2021-B.30.ATA.0.01.00/420) and study was organized within the scope of the Declaration of Helsinki. Written consent was not required as the study was based on image and data scanning.

In order to identify the patients, the data of the patients who underwent cranial MRI within the said 1-year period were searched from the database of our clinic at a single center. Among these patients, a list was created by looking at the images and choosing those with T2-SPACE images as well as conventional MR sequences. All cerebral MRI scans received were reviewed by two neuroradiologists, one with 13 years of experience and the other with 8 years of experience. Whole reports were evaluated for intraosseous AGs located in the anterior and MCF floor. Patients with intraosseous AG, all them had T2-SPACE sequence, were included in the study. The exclusion criteria were patients who could not be evaluated due to motion artifact, having additional pathology such as intracranial mass, and a history of operation and trauma. AGs adjacent to the superior sagittal sinus were also not included in the study. All cases with AG were evaluated by two radiologists (E.G. and H.O.) using the following criteria: (1) location in the anterior and MCF, (2) CSF and/or parenchyma retention, (3) exclusion of other pathologies, especially mass lesion, with standard diagnostic criteria (oval/round shape, no solid lesions enhanced in post-contrast sections, and no blooming artifacts in gradient echo (GE) sequences). In cases where the two radiologists were in conflict, consensus was established with a joint second evaluation. Demographic information of each patient was taken from our database and noted.

Imaging technique

All patients' cranial MR images obtained from 3 T MRI scan (Magnetom Skyra; Siemens Healthcare, Erlangen, Germany) using standard head coil. All imaging studies included conventional axial spin-echo (SE) T1 (TR/TE = 450/8 ms, FOV: 256 × 182 mm, slice thickness: 4 mm), coronal and sagittal turbo spin-echo (TSE) T2 (TR/TE = 3100/90 ms, FOV: 256 × 182 mm, slice thickness: 4 mm), axial fluid-attenuated inversion recovery (FLAIR) (TR/TE = 10,000/120 ms,

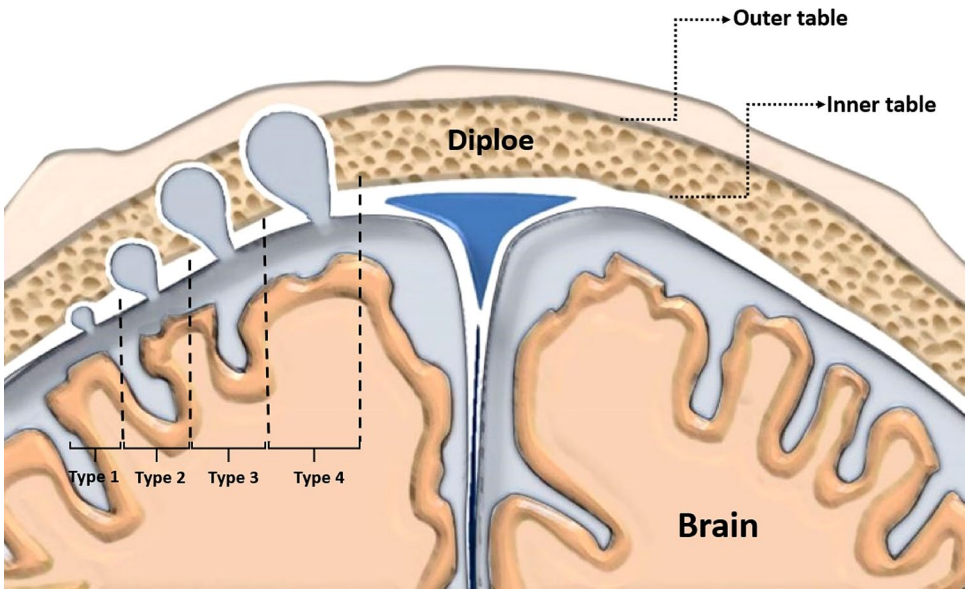

Fig. 1 The typing of intraosseous arachnoid granulations according to bone erosion

FOV: 256 × 182 mm, slice thickness: 4 mm, inversion time: 2000 ms) and sagittal plane 3D T2-SPACE sequences (T2-weighted variant flip angle mode motion-sensitive sequence; TR/TE = 3200/400 ms; FOV: 256 × 182 mm; slice thickness: 1 mm; NSA: 1; Matrix: 205 × 256; flip angle: variable). Some patients also had post-contrast T1-weighted images, contrast-enhanced MR venography images.

Imaging analysis

All available MR images were examined in high-resolution monitors and communication system (Syngo Via console, software v. 2.0; Siemens Medical Solutions, Erlangen, Germany). Consent-based analysis of all MR images was performed by two neuro radiologists. Forty-six patients with AG detected in the anterior and MCF in 485 patients T2-SPACE images scanned were included in the study. The number of AG, their location (anterior/MCF), the largest diameter in the three axes, their contents and their indentations to the bone structure were carefully examined and noted for each case. The presence of AG in the anterior and MCF was determined by scanning of the MR images. The diameter of each arachnoid granulation was grouped in the ranges of 0–2 mm, 2.1–4 mm, 4.1–6 mm, 6.1–8 mm and 8.1–10 mm. No arachnoid granulation over 8.1 mm was observed. Its contents were separated only as CSF and CSF together with brain parenchyma. Bone structure indentation was graded as grade 1 at the inner tabula, grade 2 at the diploe distance, grade 3 reaching the outer tabula, and grade 4 exceeding the outer tabula. In addition, the images of each patient were evaluated in terms of partial empty sella, edema in the optic nerve sheath, tortuosity in the optic nerve, prominence in Meckel's cave, and the presence of meningoencephalocele. Conventional MR sequences of each of the 45 patients were also evaluated randomly and independently of T2-SPACE images. The appearance features of AGs detected in anterior and MCF were determined similar to those in T2-SPACE.

Statistical analysis

SPSS program version 22 (SPSS for Windows; SPSS, Chicago, IL, USA) was used for statistical analysis. Chi-square test was used to evaluate the categorical data group. Continuous data were evaluated with the Mann–Whitney *U* test. A value of $P < 0.05$ was accepted as statistically significant.

Results

Forty-six patients, 32 of who were female, with a mean age of 46 (between 20 and 88 years) were included in the study. A total of 65 AG were examined: 1 in 35 patients, 2 in 5 patients, 3 in 4 patients, and 4 in 2 patients with 3D T2-SPACE imaging. On all the patients with AGs who had T2-SPACE sequence, AGs were related to intracranial CSF space. Patient data are summarized in Table 1.

Nineteen of the AG were located at the anterior fossa floor and 46 at the MCF floor (70%). Seventy-two percent (23/32) of patients with AG located in the MCF and 68% (9/14) of those located in the anterior fossa were female. Nineteen of the AGs were 0–2 mm, 20 of them 2.1–4 mm, 16 of them 4.1–6 mm and 10 of them 6.1–8 mm. There was no significant relationship between the sizes of AGs and the age and gender (*p*: 0.25) of patients, bone indentation (*p*: 0.179) and ICP increase signs (*p*: 0.301). All 4 AGs with parenchymal herniation were between 6 and 8 mm in size. The mean AGs size was 4.6 mm in patients with additional findings of IIH and 4.2 mm in those without.

Ten of the AGs were in the inner table, half of them in the MCF and the other half in the anterior fossa. 35 (53%) of them reached the diploe distance and 23 of them were in the MCF. Thirteen of the 15 AGs reaching the outer tabula and all 5 AGs reaching the outer tabula were located in the MCF (Figs. 2, 3). CSF leakage from ethmoid cells was observed in one patient, but this situation was not evaluated as AG. No statistical correlation could be established between bone indentation and age, gender, location, and ICP increase findings.

Twenty-five (54%) of 46 patients had at least 1 radiological finding indicating increased ICP. Eighteen of the cases were women (72%). In 22 of them, AG was located in the MCF (68%) and this was statistically significant (*p*: 0.003). The sizes of AGs in patients with signs of increased ICP were over 4.1 mm in 16 patients. Statistically, no relationship was found with size. However, 8 (80%) of 10 patients with AG greater than 6.1 mm had evidence of increased ICP (Fig. 4).

Only 4 of the AGs contained parenchyma as well as CSF. All of them were over 6.1 mm in size and were located in the MCF. In addition, all of them had accompanying signs of ICP increase (Fig. 4C, D). The mean age of

Table 1 The data of the patients are summarized in the table

Number of AG	Gender		Size of AG				Bone erosion grade				AG content		IIH sign	
	Female	Male	0–2 mm	2.1–4 mm	4.1–6 mm	6.1–8 mm	1	2	3	4	CSF	CSF + BT	Yes	No
ACF	13	6	9	4	3	3	5	12	2	–	19	–	2	17
MCF	31	15	10	16	13	7	5	23	13	5	42	4	36	10

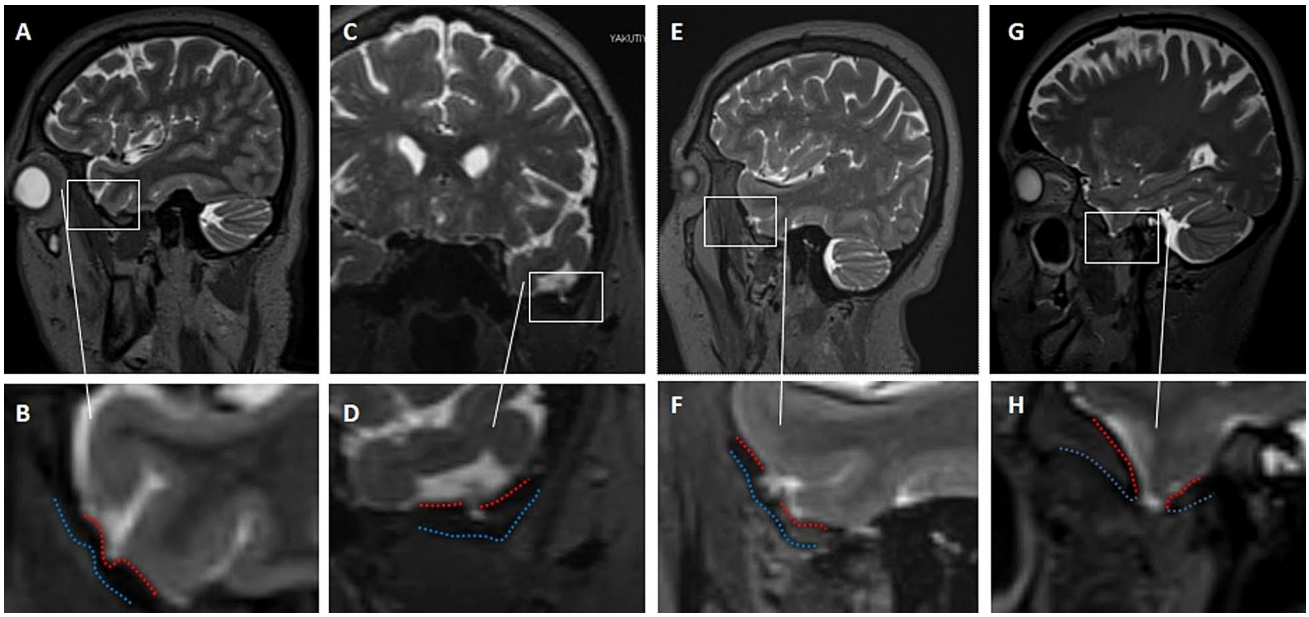

Fig. 2 The degree of indentation of arachnoid granulations to the bone structure. In grade 1 (**A**, **B**), grade 2 (**C**, **D**), grade 3 (**E**, **F**) and grade 4 (**G**, **H**) grading, the red dashed lines indicate the bone inner table and the blue ones the outer table

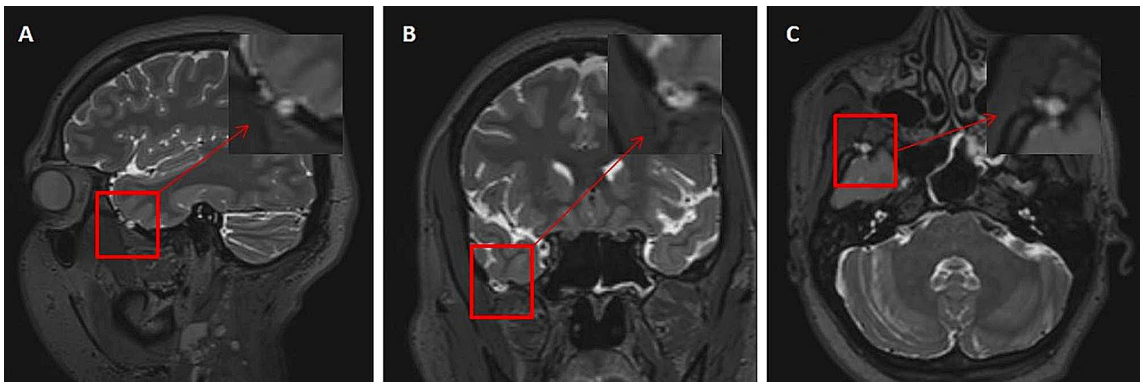

Fig. 3 T2-SPACE sagittal (**A**), coronal (**B**) and axial (**C**) sections of a 37-year-old female patient show grade 4 AG with CSF, 5.5 mm in size, in the right cranial fossa

patients with AGs containing parenchyma was 28 (20–29). In the statistical analysis, it was shown that parenchymal herniation is common in young ages (p: 0.001).

With conventional MR sequences, 17 intraosseous AG were detected in 45 patients (38%), 14 of which were in the middle and 3 were in the anterior fossa. Eight of them were 4.1–6 mm in size and 9 of them were 6.1–8 mm in size. It was determined that the content of all of them was CSF. While indentation to the bone structure was at diploe distance in 10 of them (59%), it reached the outer tabula in 7 of them (41%). When compared with T2-SPACE images, it was seen that one of the AG, which was 4.1–6 mm in size, was 6.1–8 mm in size and contained parenchyma (Fig. 5). AGs below 4 mm could not be detected with conventional sequences.

Discussion

Frequent locations of AGs that are not associated with venous sinus are shown as the anterior and MCF [14, 15]. In the literature, imaging of these areas with CT and conventional MRI sequences has been included and their relationship with IIH and CSF leaks has been investigated [6, 16–18]. This is the first study to perform a detailed

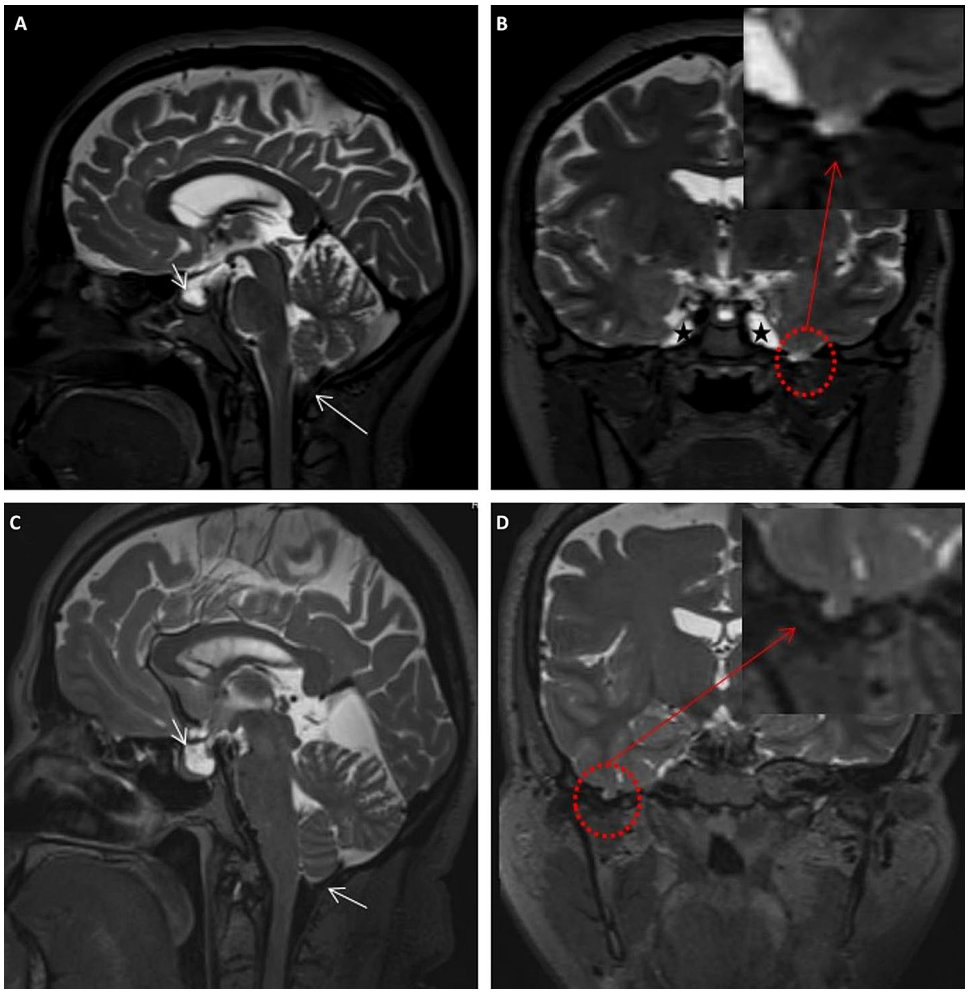

Fig. 4 Grade 4 arachnoid granulation is observed in the left MCF in the patient with extension of the PES and cerebellar tonsils to the foramen magnum (**A**, arrows). T2-SPACE images of the patient with ethmoid CSF leakage show the extension of the PES and cerebellar tonsils to the foramen magnum (**C**, arrows) and grade 2 arachnoid granulation in the right MCV (**D**)

evaluation of intraosseous AGs with 3D T2-SPACE imaging with 3 T MRI.

Three-dimensional T2-SPACE imaging is very advantageous compared to conventional sequences because it is both fast and thin-sectioned. The image quality is high as it allows the multi-planar reconstruction (MPR), as well as minimizing motion artifacts [19, 20]. The thin slices reduce the partial volume effect and prevent data loss by enabling gapless imaging. Signal to noise ratio (SNR) and contrast to noise ratio (CNR) were significantly higher in all anatomical structures in 3D T2-SPACE sequence [19]. Intraosseous AGs have been shown many times before on CT and conventional sequences. While the radiation dose in CT is an important disadvantage and it is insufficient to distinguish granulation from bone masses, especially when it is numerous. It is also very difficult to determine the granulation content with CT. Conventional brain MR imaging is traditionally performed when differential diagnosis cannot be made and to detect radiological findings of IIH. This may be insufficient to evaluate small AG due to its thick cross-section. Similar to CT, it is more difficult to determine the content of herniation in routine sequences, rather in smaller AGs [10, 21]. In our study, AGs below 4 mm could not be demonstrated with conventional sequences. When compared with T2-SPACE in larger ones, it was found to be insufficient in anatomical detailing. T2-SPACE imaging, contrary to all these disadvantages, can show each intraosseous AG in detail, from its content to the degree of bone indentation.

A number of hypotheses have been proposed in the pathogenesis of intraosseous AGs. It has been thought that conditions such as coughing and straining increase ICP intermittently, and accordingly, rupture of the arachnoid membrane causes erosion in the dura and bone in the advanced stage [6, 17, 22]. It has also been suggested that fluctuations in ICP caused by hypoxia and CSF pulsations along the MCF are factors in the pathogenesis [6, 23]. In a study on AGs causing defects in the posterior temporal bone, 76% of the patients were female (13/17) [18]. In the study of Cristopher et al. in which CT images of 1000 patients were scanned, arachnoid pits were seen five times more frequently in women [24]. In our study, the rate of women in patients with IAG was high (71%) in support of these studies. Although

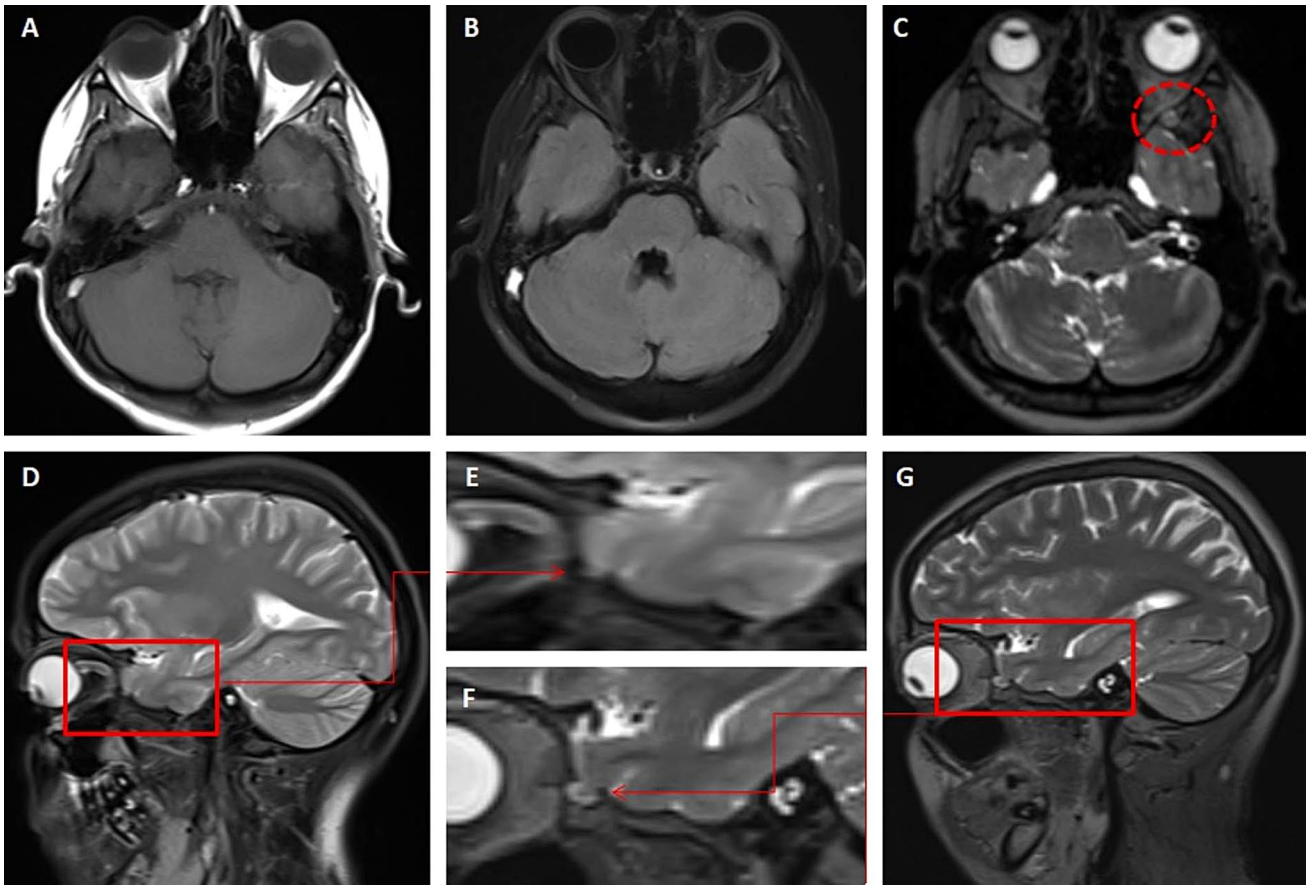

Fig. 5 While no lesion is seen in T1 (**A**) and FLAIR (**B**) weighted axial sections, AG is observed in the left MCV in the same level T2-SPACE image (**C**) (red ring). Conventional T2 (**D**, **E**) AG of the same patient was detected, but the anatomical detail is much higher in T2-SPACE sagittal sections (**F**, **G**) (color figure online)

there is no study on the distribution of intraosseous AGs in the entire calvarium, it has been reported that they are common in the anterior and MCF. In our study, 70% of AGs were in the MCF. This can be explained by the higher pressure in the MCF, which supports the hypotheses of the AG's formation mechanism.

Idiopathic intracranial hypertension, also called pseudotumor cerebri, is defined as an increase in ICP when CSF is normal and hydrocephalus is absent [22, 25]. Obesity and being female patient are important predisposing factors. The diagnosis is made by lumbar puncture when the ICP pressure is above 25 cm H_2O. However, in clinically suspected cases, MR findings help to establish the diagnosis. The cause of the disease has been fully revealed. However, there is a hypothesis that AGs in the dural sinuses may play a role in the pathogenesis [16]. In addition, intraosseous AGs are considered as a result of IIH and are counted as MR findings [17]. Other findings include tortuosity in the optic nerve, enlargement of the optic nerve sheath, scleral flattening, enlargement of Meckel's caves, dural ectasia, and meningoencephalocele. Spontaneous CSF leaks are also thought to be associated with IIH. In a study on MR findings of patients with spontaneous and non-spontaneous ethmoidal CSF leakage, arachnoid pits were found to be the most common IIH finding in spontaneous patients [26]. In another study examining spontaneous sphenoid sinus CSF leaks, arachnoid pits were detected in 63% of the patients (7/11) and AG was not found in the control group. In the investigation of 14 patients with spontaneous CSF leakage, 11 of the cases had arachnoid pits, while in 2 of them arachnoid pits were the only finding supporting IIH. Measurement of CSF could not be made in 3 of 11 patients, but it was either borderline elevation or increased in eight patients [6]. In the study of Cristopher et al., while 234/1000 patients had AG, CSF leakage associated with the sphenoid sinus was detected in seven of them. In the general population, the rate of intraosseous AG was lower in ours (9, 46/485). We thought that this was due to the distribution inequality of the patients. The fact that 54% of the patients had at least one additional MRI finding supporting IIH and that the majority of these patients (72%) were women suggest

that AGs are an important finding of IIH. In our study, we showed that the MCF location of the AG supports IIH more than its anterior location. Of the 19 patients with no other sign of IIH other than arachnoid granulation, 68% were women. This may suggest that the definitive diagnosis of IHH cannot be made here. Arachnoid granulations, especially seen in MCF, may be precursor lesions indicating IIH. In order to determine this, studies with a wide spectrum of patient follow-up are required.

It has been shown that when intraosseous AG encounter the air-filled space (such as the sphenoid sinus, ethmoid cells, and mastoid bone) and completely erode the bone, it causes CSF leakage [15, 18]. Studies have determined that the number and size of AGs increase with age. Therefore, radiological reporting and follow-up of AGs, especially adjacent to air spaces, is required for possible CSF leaks. But it is argued that AGs that are not associated with the air gap have no clinical significance [18, 27]. In our four patients, AGs completely eroded the bone structure and parenchyma was present in the herniation. The mean age of these patients also included the young population. Although they are far from the air spaces, we think that the presence of parenchyma may cause possible microdamage. It has been previously shown that giant AGs (over 1 cm) within the venous structure have pathological signal intensities suggestive of parenchymal damage [28]. All our cases were smaller than 8 mm in size and possible damage may not have been reflected in imaging. Therefore, detailed evaluation of AGs is important not only for possible CSF leaks, but also for the determination of parenchymal herniation.

Our study had some limitations. The first of these was because it was retrospective. Although we consider IIH and show AGs in the patients, the diagnosis was not confirmed by lumbar puncture. In addition, none of the AG were diagnosed histopathologically. Finally, it was difficult to determine the degree of indentation of AG to the bone structure, especially at the level of ethmoid cells, where the bone structure is thin.

As a result, the identification and detailed evaluation of intraosseous AG located in anterior and MCF can be done easily, safely and effectively with T2-SPACE imaging. Their determination, especially in MCF, can be a strong indicator of an increase in ICP. At the same time, with the detection of AGs, both possible CSF leaks and parenchymal herniation can be determined.

Declarations

Conflict of interest There is no conflict of interest.

References

1. Leach JL, Jones BV, Tomsick TA et al (1996) Normal appearance of arachnoid granulations on contrast-enhanced CT and MR of the brain: differentiation from dural sinus disease. AJNR Am J Neuroradiol 17:1523–1532
2. Le Gros Clark WE (1920) On the Pacchionian bodies. J Anat 55:40–48
3. VandeVyver V, Lemmerling M, De Foer B et al (2007) Arachnoid granulations of the posterior temporal bone wall: imaging appearance and differential diagnosis. AJNR Am J Neuroradiol 28:610–612
4. Kaufman B, Nulsen FE, Weiss MH et al (1977) Acquired spontaneous, nontraumatic normal-pressure cerebrospinal fluid fistulas originating from the middle fossa. Radiology 122:379–387
5. Leach JL, Meyer K, Jones BV et al (2008) Large arachnoid granulations involving the dorsal superior sagittal sinus: findings on MR imaging and MR venography. AJNR Am J Neuroradiol 29:1335–1339
6. Shetty PG, Shroff MM, Fatterpekar GM, Sahani DV, Kirtane MV (2000) A retrospective analysis of spontaneous sphenoid sinus fistula: MR and CT findings. AJNR Am J Neuroradiol 21(2):337–342
7. Schmalfuss IM, Camp M (2008) Skull base: pseudolesion or true lesion? Eur Radiol 18:1232–1243
8. Suzuki H, Takanashi J, Kobayashi K et al (2001) MR imaging of idiopathic intracranial hypertension. AJNR Am J Neuroradiol 22:196–199
9. Trimble CR, Harnsberger HR, Castillo M, Brant-Zawadzki M, Osborn (2010) Giant arachnoid granulations just like CSF?: NOT!! AG AJNR Am J Neuroradiol. 31(9):1724–1728
10. Lu CX, Du Y, Xu XX et al (2012) Multiple occipital defects caused by arachnoid granulations: Emphasis on T2 mapping. World J Radiol 4(7):341–344. https://doi.org/10.4329/wjr.v4.i7.341
11. Mugler JP, Bao S, Mulkern RV et al (2000) Optimized single-slab three-dimensional spin-echo MR imaging of the brain. Radiology 216:891–899
12. Ogul H, Guven F, Izgi E, Kantarci M (2019) Evaluation of giant arachnoid granulations with high-resolution 3D-volumetric MR sequences at 3T. Eur J Radiol 121:108722
13. Kannath SK, Alampath P, Enakshy Rajan J et al (2016) Utility of 3D SPACE T2- weighted volumetric sequence in the localization of spinal dural arteriovenous fistula. J Neurosurg Spine 25:125–132
14. Chen F, Deng XF, Liu B, Zou LN, Wang DB, Han H (2011) Arachnoid granulations of middle cranial fossa: a population study between cadaveric dissection and in vivo computed tomography examination. Surg Radiol Anat 33(3):215–221. https://doi.org/10.1007/s00276-010-0733-2
15. Gacek RR, Gacek MR, Tart R (1999) Adult spontaneous cerebrospinal fluid otorrhea: diagnosis and management. Am J Otol 20:770–776
16. Watane GV, Patel B, Brown D, Taheri MR (2018) The significance of arachnoid granulation in patients with idiopathic intracranial hypertension. J Comput Assist Tomogr 42(2):282–285
17. Silver RI, Moonis G, Schlosser RJ, Bolger WE, Loevner LA (2007) Radiographic signs of elevated intracranial pressure in idiopathic cerebrospinal fluid leaks: a possible presentation of idiopathic intracranial hypertension. Am J Rhinol 21(3):257–261. https://doi.org/10.2500/ajr.2007.21.3026
18. Lee MH, Kim HJ, Lee IH, Kim ST, Jeon P, Kim KH (2008) Prevalence and appearance of the posterior wall defects of the temporal bone caused by presumed arachnoid granulations and

their clinical significance: CT findings. AJNR Am J Neuroradiol 29(9):1704–1707
19. Hossein J, Fariborz F, Mehrnaz R, Babak R (2018) Evaluation of diagnostic value and T2-weighted three-dimensional isotropic turbo spin-echo (3D-SPACE) image quality in comparison with T2-weighted two-dimensional turbo spin-echo (2D-TSE) sequences in lumbar spine MR imaging. Eur J Radiol Open 28(6):36–41. https://doi.org/10.1016/j.ejro.2018.12.003
20. Kloth JK, Winterstein M, Akbar M, Meyer E, Paul D, Kauczor HU (2014) Comparison of 3D turbo spin-echo SPACE sequences with conventional 2D MRI sequences to assess the shoulder joint. Eur J Radiol 83(10):1843–1849
21. Park SH, Park KS, Hwang JH (2018) Arachnoid granulations mimicking multiple osteolytic bone lesions in the occipital bone. Brain Tumor Res Treat 6(2):68–72. https://doi.org/10.14791/btrt.2018.6.e8
22. Wall M (1991) Idiopathic intracranial hypertension. Neurol Clin 9:73–95
23. Clark D, Bullock P, Hui T et al (1994) Benign intracranial hypertension: a cause of CSF rhinorrhea. J Neurol Neurosurg Psychiatr 57:847–849
24. Barañano CF, Curé J, Palmer JN, Woodworth BA (2009) Sternberg's canal: fact or fiction? Am J Rhinol Allergy 23(2):167–171. https://doi.org/10.2500/ajra.2009.23.3290
25. Wessel K, Thron A, Linden D et al (1987) Pseudotumor cerebri: clinical and neuroradiological findings. Eur Arch Psychiatr Neurol Sci 237:54–60
26. Peker E, Kuru Öz D, Kul M, Erdoğan M, Öztuna D, Erden Mİ (2018) Neuro-ophthalmologic MRI findings in the detection of rhinorrhoea aetiology. Neuroophthalmology 43(4):244–249. https://doi.org/10.1080/01658107.2018.1540643
27. Grossman CB, Potts DG (1974) Arachnoid granulations: radiology and anatomy. Radiology 113:95–100
28. Gozgec E, Ogul H, Izgi E, Kantarci M (2021) Tissue damage in herniated brain parenchyma into giant arachnoid granulations: demonstration with high resolution MRI. Acta Radiol 62(6):799–806. https://doi.org/10.1177/0284185120941829